

Electronic Supplementary Information

For

Multicolor colorimetric detection of dopamine based on iodide-responsive copper-gold nanoparticles

Yufeng Sun^{a,b,‡}, Minjie Peng^{a,‡}, Aiguo Wu^{a,c}, Yujie Zhang^{a,c*}

^a Cixi Institute of Biomedical Engineering, International Cooperation Base of Biomedical Materials Technology and Application, CAS Key Laboratory of Magnetic Materials and Devices and Zhejiang Engineering Research Center for Biomedical Materials, Ningbo Institute of Materials Technology and Engineering, Chinese Academy of Sciences (CAS), Ningbo Key Laboratory of Biomedical Imaging Probe Materials and Technology, Ningbo 315201, China

^b Faculty of Materials, Metallurgical and Chemistry, Jiangxi University of Science and Technology, Ganzhou 341000, China.

^c University of Chinese Academy of Sciences, Beijing 100049, China

* Corresponding Authors

Tel: 0086-574-86685513; Fax: 0086-574-63875029; Email: zhangyujie@nimt
e.ac.cn

‡ Y.S. and M.P. contributed equally to this work.

Table of Content

Table S1. DA determination in real samples.....	S3
Section 1. Materials and characterization.....	S4
Section 2. Preparation of Cu-Au NPs.....	S5
Section 3. Colorimetric detection of DA.....	S5
Section 4. Selectivity of DA detection probe	S5
Section 5. Colorimetric detection of DA in urine/serum.....	S6
Figure S1. Characterization of nanoparticles... ..	S7
Figure S2. Wide scan XPS spectra of Cu-Au NPs, Cu-Au NPs with KI and Cu-Au NPs with DA and KI.	S8
Figure S3. UV-vis absorption spectra and photographs of Au NPs solutions under different conditions.	S9
Figure S4. Effect of I ⁻ concentration on the detection of DA.	S10
Figure S5. Effect of pH value on the detection of DA.....	S11
Figure S6. Effect of time on DA detection.	S12
Figure S7. Selectivity of DA detection probe based on Cu-Au NPs.	S13
Figure S8. Anti-interference of DA detection probe based on Cu-Au NPs.	S14
Figure S9. Absorbance ratios of Cu-Au NPs solutions in the absence and presence of DA at different time.....	S15
Figure S10. Image of the Cu-Au NPs with DA from 0.05 to 5 μ M.....	S16
Figure S11. TEM imagines of Cu-Au NPs with different concentrations of DA and I ⁻	S17
Ethical approval	S18
References	S18

Table S1. DA determination in real samples

Samples	Spiked concentration (μM)	Measured by HPLC (μM)	Measured by this probe (μM)	Recovery (%)
Urine	20	20.18 \pm 0.014	19.58 \pm 0.014	97.03
	30	29.96 \pm 0.020	30.88 \pm 0.050	103.07
	40	40.60 \pm 0.23	38.51 \pm 0.013	94.85
FBS	25	24.78 \pm 0.0071	23.56 \pm 0.022	95.08
	30	30.36 \pm 0.019	30.63 \pm 0.13	100.89
	40	40.97 \pm 0.25	39.19 \pm 0.0055	95.66

Section 1. Materials and characterization

Gold chloride trihydrate ($\text{HAuCl}_4 \cdot 3\text{H}_2\text{O}$), copper sulphate pentahydrate ($\text{CuSO}_4 \cdot 5\text{H}_2\text{O}$), copper chloride (CuCl_2), calcium chloride (CaCl_2), hydrochloric acid (HCl), and nitric acid (HNO_3) were purchased from Sinopharm Chemical Reagent Co. Ltd (Shanghai, China). Sodium borohydride (NaBH_4), dopamine (DA), L-isoleucine (L-Ile), D-aspartic acid (D-Asp), L-tryptophan (L-Trp), L-valine (L-Val), L-glutamic acid (L-Glu), glycine (Gly), L-serine (L-Ser), L-threonine (L-Thr), L-leucine (L-Leu), L-proline (L-Pro), L-alanine (L-Ala), L-methionine (L-Met), L-Phenylalanine (L-Phe), L-Cysteine (L-Cys), L-Lysine (L-Lys), L-Histidine (L-His), L-Arginine (L-Arg), ascorbic acid (AA), glucose (Glc), and Urea were purchased from Aladdin Reagent Co., Ltd. (Shanghai, China). Tyrosine (Tyr), Levodopa (L-DOPA), epinephrine (EPI) and norepinephrine (NE) were obtained from Maclin Biochemical Technology Co., Ltd. (Shanghai, China). L-Glutamine (L-Glu) and L-Asparagine (L-Asp) were purchased from Scientific Phygene Co., Ltd. (Shanghai, China). Trisodium citrate dihydrate ($\text{C}_6\text{H}_5\text{Na}_3\text{O}_7$) was bought from Titan Scientific Co., Ltd. (Shanghai, China). All of the chemicals were used as received without further purification. Mill-Q water (18 M Ω cm resistance) was used to prepare all the solutions in this work. All glassware was washed with aqua regia [$\text{HCl} / \text{HNO}_3 = 3:1$ (v/v)] and then rinsed with Milli-Q water.

The morphology, X-ray energy dispersive spectroscopy and element mapping were obtained by transmission electron microscopy (TEM, Hitachi HT7800 and EDX, Thermo Fisher Talos F200X). X-ray photoelectron spectroscopy (XPS, Axis Ultra DLD with Mg $\text{K}\alpha$ radiation as X-ray source) was used to analyze the chemical compositions and element states of the samples. XPS results were collected in the form of binding energy and fitted by using nonlinear least-squares curve fitting program (CasaXPS software). The solutions for analysis were coated onto silicon substrates respectively and dried for XPS analysis. Ultraviolet-Visible (UV-vis, PERSEE T10CS) absorption spectra of nanoparticles solutions were the key for the qualitative and quantitative analysis of DA. Hydrodynamic diameter and zeta potential (Malvern Zetasizer Nano ZS) were used to demonstrate the mechanism of colorimetric detection of DA. The

concentration of DA in actual urine/serum was measured using HPLC to verify the accuracy of the colorimetric probe assay.

Section 2. Preparation of Cu-Au NPs

Cu-Au NPs were generated, according to a review of the literature.¹ The specific preparation is as follows: at room temperature, 50 μL $\text{CuSO}_4 \cdot 5\text{H}_2\text{O}$ (100 mM) and 50 μL $\text{C}_6\text{H}_5\text{Na}_3\text{O}_7$ (100 mM) solutions were added to 20 mL of ultrapure water. The mixture was then swiftly injected with 1 mL of newly made NaBH_4 solution (7.6 mg NaBH_4 dissolved in 4 mL H_2O) and rapidly swirled. When the appearance of the solution transformed from dark orange to green (about 15~20 min), 100 μL aqueous solution of $\text{HAuCl}_4 \cdot 3\text{H}_2\text{O}$ (50 mM) was added and the solution was still stirred. The reaction was allowed to run at room temperature for 1 h, during which time the color of the mixture shifted from green to gray-blue. Cu-Au NPs solution was kept at room temperature (25 ± 2 °C) before use.

Section 3. Colorimetric detection of DA

800 μL of Cu-Au NPs solution and 50 μL of DA solution in various concentrations were combined, and 50 mL of HCl (2 mM) was added to the mixture to correct the pH. Then, 100 μL of KI aqueous solution (100 μM) was added into the mixed solution, resulting in a final volume of 1 mL. The UV-vis absorption spectra and color change after 15 minutes were recorded for quantitative analysis.

Section 4. Selectivity of DA detection probe

In the practical application of colorimetric detection probes, the impact of other ions or organic compounds in urine/serum on DA detection should be taken into consideration. To evaluate the selectivity of DA probe, the detection method was used to test 28 other components including Cu^{2+} , Ca^{2+} , various amino acids, AA, Glc, Urea, L-DOPA, EPI and NE (The interfering material solutions were created by dissolving each analytical purity component separately in pure water). In this study, the DA concentration in the detection system was 5 μM and that of all interfering substances

was also 5 μM), the interference of L-DOPA (10 μM), EPI (10 μM), and NE (10 μM) with biologically levels on the detection of DA was also examined. Similarly, the color and UV-vis absorption spectra of Cu-Au NP solutions were recorded. In addition, interference test was also performed, interfering substances were mixed with DA and the above detection process was repeated.

Section 5. Colorimetric detection of DA in urine/serum

Urine samples from healthy adult volunteers and fetal bovine serum (FBS) specimens were centrifuged for 30 minutes at 5000 rpm using 30 KD ultrafiltration tubes and the process was repeated twice. The filtrate was filtered via a needle membrane filter with 0.22 μm pore size. Prior to analysis, all samples were diluted, and then DA solutions of various standard amounts were added to the biological samples listed above. Subsequently, the above colorimetric detection method and HPLC were used for DA detection in these samples.

As illustrated in Figure S1a (ESI[†]), the prepared Cu-Au NPs are interconnected chain-like irregular nanoparticles with a certain degree of agglomeration. The valence states of Cu and Au were analyzed using XPS and the results are shown in Figure S1b and S1c (ESI[†]), where the binding energies of Cu 2p and Au 4f correspond to zero-valence Cu and Au respectively. From the EDS mapping in Figure S1d (ESI[†]), it can be seen that the nanoparticles are composed of two elements, namely Au and Cu, and they have no obvious core-shell structure. It can be speculated that these two elements are in the doping state. Pure Cu-Au NPs solution is gray with a broad UV-Vis absorption peak. After the addition of I⁻, the color of the solution altered from gray to pink and a more visible absorption peak emerged at 525 nm (as shown in Figure S1e, ESI[†]). This is similar to the results in the literature¹, that is, Cu-Au NPs can respond specifically to iodide.

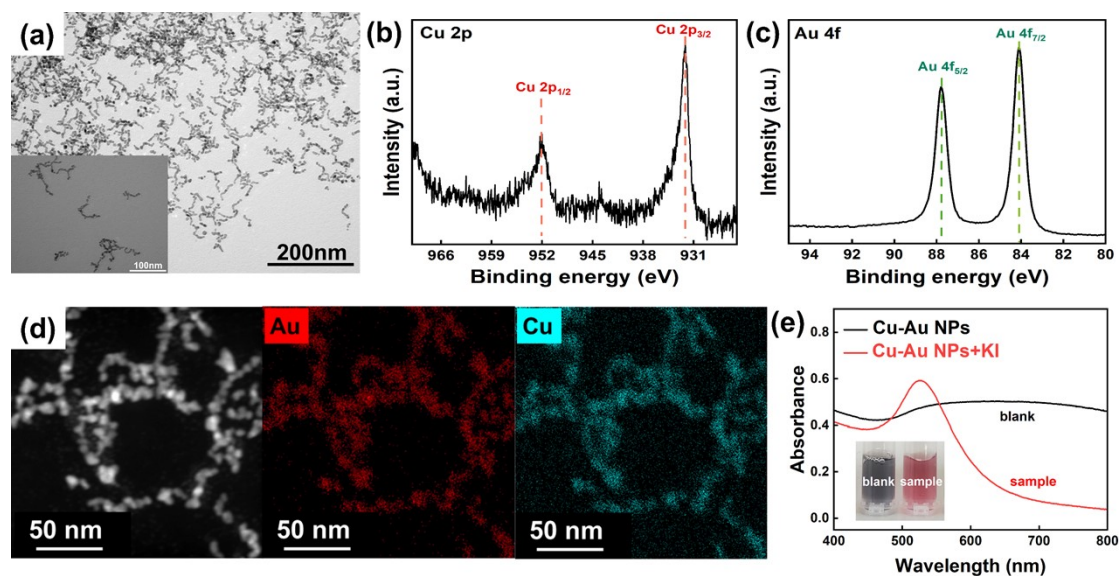


Figure S1. Characterization of nanoparticles. (a) TEM image of Cu-Au NPs; (b) Cu 2p and (c) Au 4f XPS spectra of Cu-Au NPs; (d) EDS mapping of Cu-Au NPs; (e) UV-vis absorption spectra and photographs of Cu-Au NPs solutions in the absence (black line) and presence (red line) of I⁻.

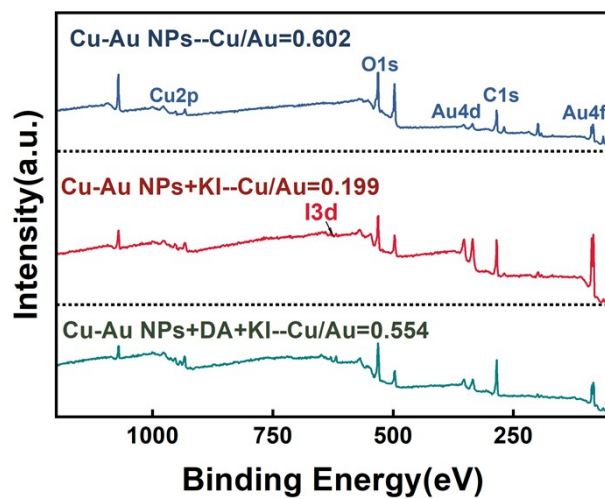


Figure S2. Wide scan XPS spectra of Cu-Au NPs, Cu-Au NPs with KI and Cu-Au NPs with DA and KI.

Au NPs did not recognize I⁻ and even though the color of the solution deepened to some extent after the addition of DA, the color change spanned a smaller range compared with that of Cu-Au NPs system.

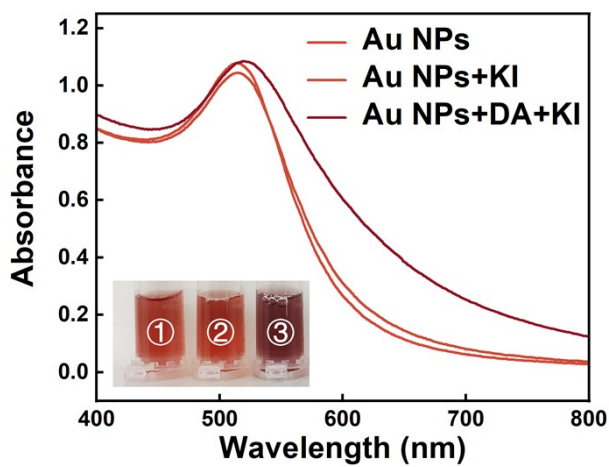


Figure S3. UV-vis absorption spectra and photographs of Au NPs solutions under different conditions (①Au NPs, ②Au NPs with KI, ③Au NPs with DA and KI).

First of all, the detection system mainly relies on the competitive adsorption of DA and I^- , therefore I^- concentration affects the detection of DA to some extent. Figure S4 (ESI†) shows the effect of I^- concentration on DA detection. The response of I^- to Cu-Au NPs was not significant when the concentration of KI is too low, at which point the presence or absence of DA had minor effect on the solution color. When the concentration of I^- raised to a certain critical value (100 μM), the response of I^- to Cu-Au NPs reached saturation, and the absorbance ratio A/A_0 of experimental group and blank group reached the maximum (where A is the absorbance ratio of probe solution at 600 nm and 525 nm in the presence of DA and KI, and A_0 denotes the absorbance ratio of blank group). At this point, the further increase of I^- concentration has no significant influence on the color and absorbance ratio of Cu-Au NPs solution. Hence, the optimal I^- concentration in DA detection system is 100 μM .

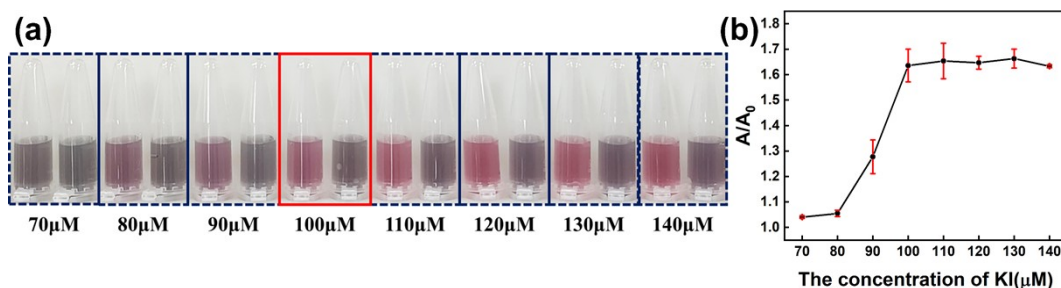


Figure S4. Effect of I^- concentration (70, 80, 90, 100, 110, 120, 130, 140 μM) on the detection of DA. (a) Colorimetric photograph; (b) UV-vis absorption intensity ratio of Cu-Au NPs solutions with DA and different concentrations of KI (A represents the absorption intensity ratio of Cu-Au NPs solution containing DA and I^- at 600 nm and 525 nm, A_0 represents the absorption intensity ratio of the blank group).

pH value not only affects the oxidation of I⁻ to iodine atoms, but also affects the protonation degree of DA, thus having an impact on the effect of DA detection. As shown in Figure S5 (ESI[†]), when the acidity of Cu-Au NPs solution is too high, the reaction between I⁻ and probe is strong, the protective effect of DA on Cu-Au NPs was restricted and the solution color of the experimental group takes on a purple hue. When Cu-Au NPs solution is neutral and alkaline, the oxidation of I⁻ was affected, Cu-Au NPs were not completely decomposed and reorganized, and the color of the blank groups takes on an incomplete pink. When 2 mM HCl was added, the variation in color between the blank and experimental groups was the greatest, DA detection effect was the strongest, and the result was consistent with that of UV-vis absorption spectra data.

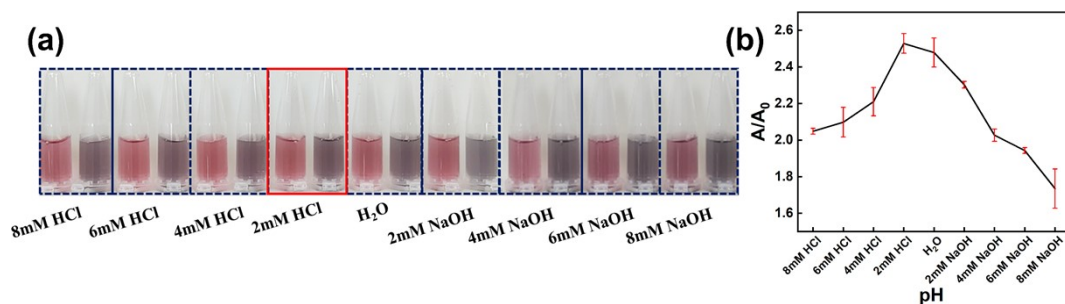


Figure S5. Effect of pH value (8, 6, 4, 2 mM HCl, H₂O, 2, 4, 6, 8 mM NaOH) on the detection of DA. (a) Photograph of the colorimetric results; (b) UV-vis absorption intensity ratio of Cu-Au NPs solutions with different pH value.

The effect of the incubation time between DA and Cu-Au NPs and reaction time between I^- and nanoparticles on DA detection were investigated when other detection conditions were optimal. Figure S6a (ESI†) shows the relationship between incubation time (DA and Cu-Au NPs) before I^- addition and absorbance ratio $A_{600\text{nm}}/A_{525\text{nm}}$ of Cu-Au NPs system. It should be noted that the final results reveal that the incubation time is not related to DA detection. Afterwards, the trend of the absorbance ratio A/A_0 between 3 ~ 30 min after the addition of I^- was investigated, as shown in Figure S6b (ESI†). It is clear that the ratio of A/A_0 tends to be stable when the reaction time reached 15 min, which indicated that the reaction was basically completed at this point. As a result, 15 min was selected as the optimal reaction time. The fact that the detection method does not require special incubation makes it significantly faster than other colorimetric detection methods².

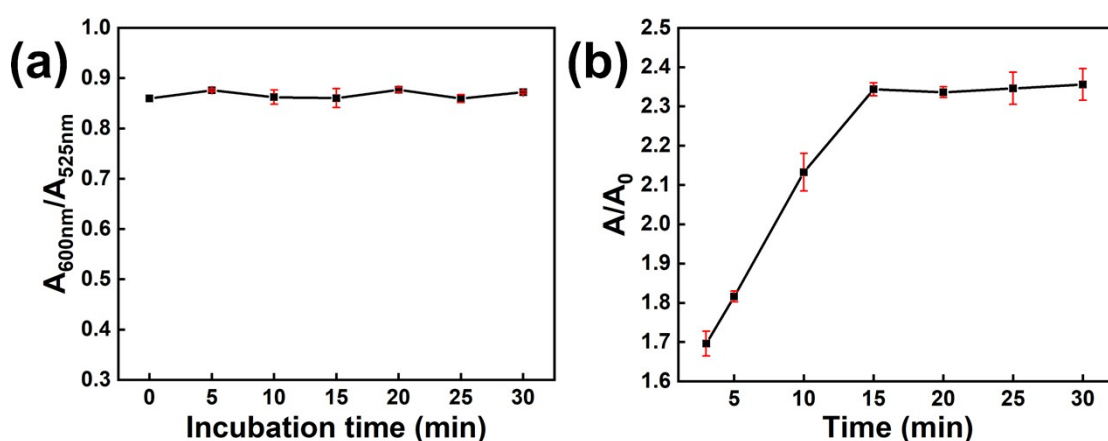


Figure S6. Effect of time on DA detection. (a) Ratio of absorbance intensity at 600 nm and 525 nm for Cu-Au NPs solutions with different incubation time between DA and Cu-Au NPs; (b) The relationship between the reaction time (I^- and Cu-Au NPs) and absorbance ratio.

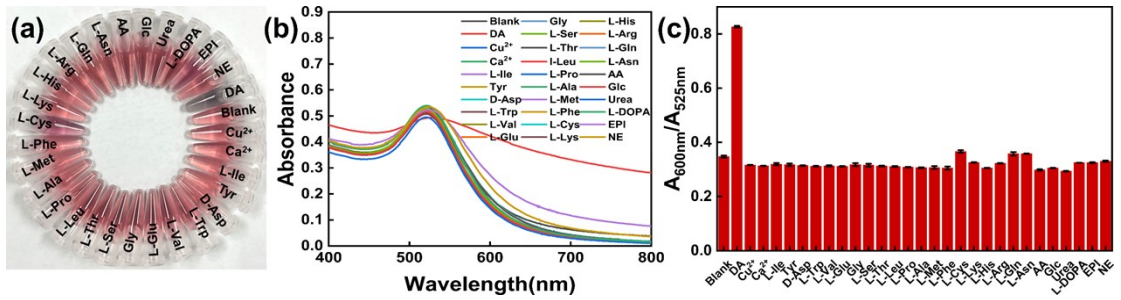


Figure S7. Selectivity of DA detection probe based on Cu-Au NPs. (a) Colorimetric picture, (b) UV-vis absorption spectra and (c) UV-vis absorbance ratios ($A_{600\text{nm}}/A_{525\text{nm}}$) of Cu-Au NPs solutions with I⁻ in the presence of DA or other interferences.

Due to the coexistence of multiple components in the actual samples, it is also essential to study whether other components in urine/serum interfere with DA detection. Other ingredients were mixed with DA to obtain the mixed solution for the experiment, and the mixed solutions reacted with DA detection probe. The concentration of DA, the type and concentration of interfering components used in the mixed solution are the same as those in the selectivity experiment. The colorimetric photograph (Figure S7a, ESI†) shows that only the blank group is pink in color. As long as DA exists, Cu-Au NPs colorimetric probe solutions remained gray. Similarly, only the UV-vis absorption spectrum of the blank group has a prominent absorption peak at 525 nm, while the absorbance curves of all other Cu-Au NPs solutions containing DA and other interfering components are relatively flat (Figure S7b, ESI†) and the trend is very similar to that of Cu-Au NPs solution containing only DA. Figure S7c (ESI†) obtained by processing the data in Figure S7b shows that the absorption ratios $A_{600\text{nm}}/A_{525\text{nm}}$ of Cu-Au NPs colorimetric probe solutions containing DA are greater than that of the blank sample, and the values are very close. Therefore, other interfering components have no influence on the detection of DA. To sum up, Cu-Au NPs colorimetric detection probe shows excellent anti-interference ability.

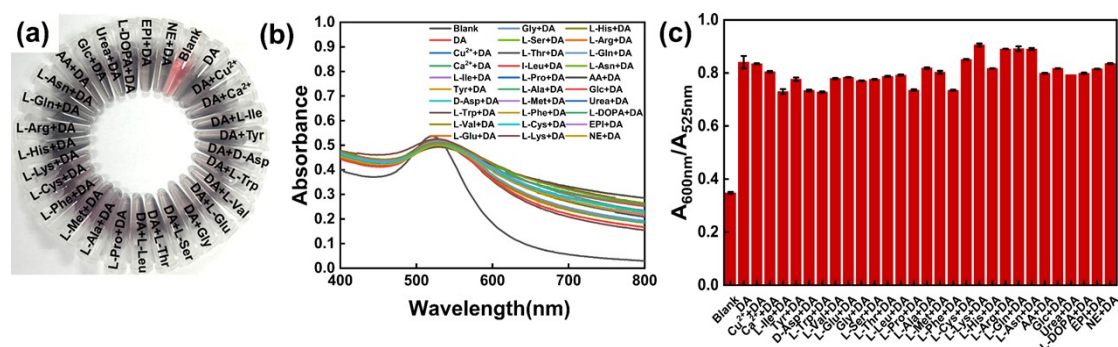


Figure S8. Anti-interference of DA detection probe based on Cu-Au NPs. (a) Colorimetric photograph, (b) UV-vis absorption spectra, and (c) UV-vis absorbance ratios ($A_{600\text{nm}}/A_{525\text{nm}}$) of Cu-Au NPs solutions containing mixture of DA and other components.

To test the stability of colorimetric detection probe for DA, the prepared Cu-Au NPs were employed for colorimetric detection of DA with the same concentration for 30 consecutive days (DA solutions were prepared every day because DA would self-aggregate). Figure S8 (ESI†) shows the absorbance ratios $A_{600\text{nm}}/A_{525\text{nm}}$ of the blank and experimental groups within 30 days. The results show that the nanoparticles were the most stable after 5 days with a small fluctuation. The detection results have a relative standard deviation (RSD) of 12.7%, indicating that the detection method has good stability.

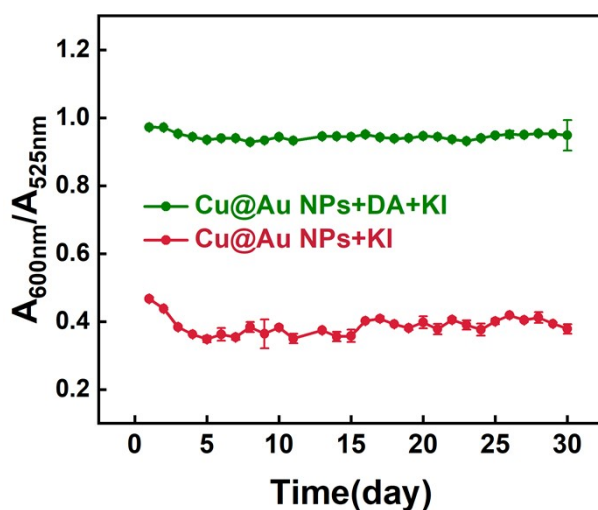


Figure S9. Absorbance ratios of Cu-Au NPs solutions in the absence and presence of DA at different time.



Figure S10. Image of the Cu-Au NPs with DA from 0.05 to 5 μM.

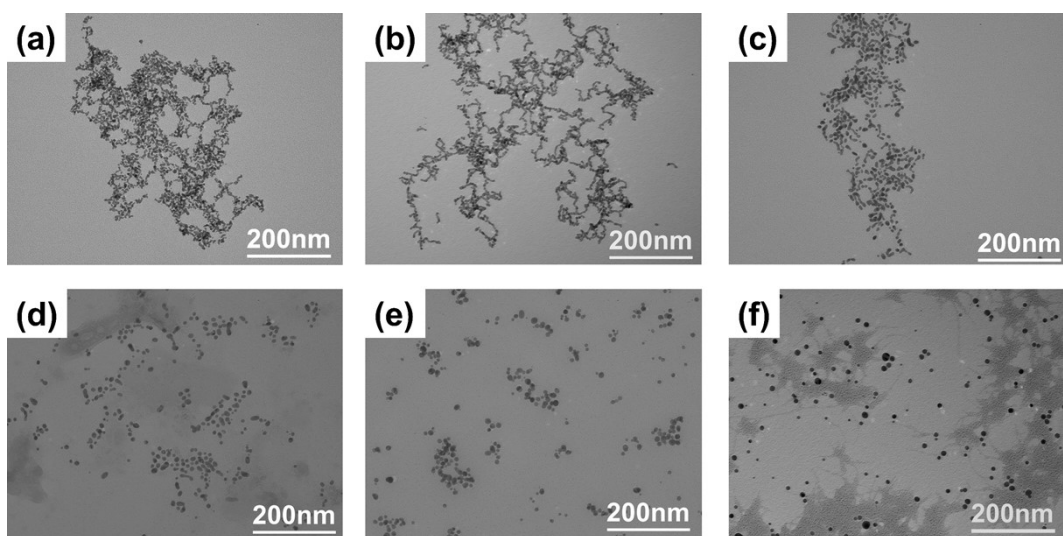


Figure S11. TEM images of Cu-Au NPs with different concentrations of DA and I⁻ (a) Cu-Au NPs; (b) Cu-Au NPs with 20 μM DA and I⁻; (c) Cu-Au NPs with 10 μM DA and I⁻; (d) Cu-Au NPs with 2 μM DA and I⁻; (e) Cu-Au NPs with 1 μM DA and I⁻ and (f) Cu-Au NPs with 0 μM DA and I⁻.

Ethical approval

All experiments were performed in accordance with the Helsinki Guidelines and were approved by the Ethics Committee at Ningbo Institute of Materials Technology and Engineering, Chinese Academy of Sciences. Informed consent was obtained from all human subjects.

References

1. J. Zhang, X. Xu, C. Yang, F. Yang and X. Yang, *Anal. Chem.*, 2011, **83**, 3911-3917.
2. X. Fang, H. Ren, H. Zhao and Z. Li, *Microchim. Acta*, 2016, **184**, 415-421.